Studies on Solvent Evaporation and Polymer Precipitation Pertinent to the Formation of Asymmetric Polyetherimide Membranes

ROBERT Y. M. HUANG* and XIANSHE FENG

Department of Chemical Engineering, University of Waterloo, Waterloo, Ontario N2L 3G1, Canada

SYNOPSIS

The characteristics of solvent evaporation and polymer precipitation during the formation of asymmetric aromatic polyetherimide (PEI) membranes via the dry/wet phase inversion method are studied and the results are discussed with reference to membrane preparation. It is shown that the solvent evaporation from the surface of freshly cast films in early evaporation stages can be quantified by an empirical equation with two parameters. Analysis of the evaporation parameters partially explains the interaction effect of membrane preparation variables on membrane performance. The phase separation data for systems PEI/DMAc/H_2O and PEI/NMP/H_2O with and without $LiNO_3$ additive are determined using the turbidimetric titration method. The kinetic data on solvent–nonsolvent exchange and additive leaching during polymer precipitation in nonsolvent water are measured. The results presented here offer a qualitative basis for the development of asymmetric PEI membranes. © 1995 John Wiley & Sons, Inc.

INTRODUCTION

Aromatic polyetherimide (PEI), constituting the repeat unit shown, is an attractive polymeric membrane material because of its excellent thermal, chemical, and mechanical stabilities as well as its good film forming properties. The good processibility of the imide polymer can be said to be caused by the flexible ether linkage. This polymer has been used to produce membranes, in an integral or a composite form, for gas–gas separations,[1,2] organic vapor–gas separations,[3-5] and pervaporation separations of liquid mixtures.[6-9] Because membrane separation is a rate-governed separation process, almost all commercially important membranes are structurally asymmetric in order to ensure high productivity.

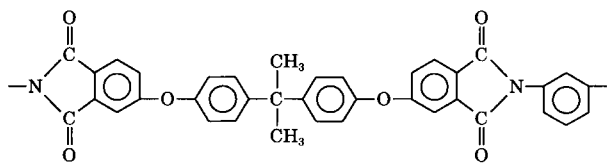

* To whom correspondence should be addressed.

Journal of Applied Polymer Science, Vol. 57, 613–621 (1995)
 CCC 0021-8995/95/050613-09

The integral asymmetric membranes, consisting of a dense skin layer supported on a microporous substrate, are normally prepared via the phase inversion process, during which both membrane layers are formed from a single polymer solution. A well-known example of such a membrane is the asymmetric cellulose acetate membrane developed by Loeb and Sourirajan for water desalination by reverse osmosis.[10] However, it was noticed that the asymmetric reverse osmosis membranes produced by the classical phase inversion method are generally unsuitable for pervaporation separations.[11] Nevertheless, in our previous studies asymmetric aromatic PEI membranes were prepared by the dry/wet phase inversion technique; these membranes were shown to be promising for the separation of water from isopropanol by pervaporation.[6,7] Studies on the effects of membrane casting conditions upon the membrane performance have shown that both the dry (partial evaporation of solvent) and the wet (immersion precipitation of polymer) steps involved in the procedure for membrane preparation influence the pervaporation properties of the resultant membranes significantly.[8] A study of both steps to precisely define and control the membrane casting

conditions is therefore needed for the membrane development.

There are several theoretical models proposed to describe the solvent evaporation pertinent to the dry step during the formation of asymmetric membranes,[12-15] but no reliable predictions of the solvent evaporation rate have been made. Relatively few experimental investigations on solvent evaporation have been reported, and the experimental work has been concerned primarily with cellulose acetate/acetone solutions.[15-17] As far as polymer precipitation in a nonsolvent is concerned, the equilibrium phase separation data for polymer–solvent–nonsolvent systems are frequently used at present to get some insight into polymer precipitation from the thermodynamic point of view. However, the membrane structure is influenced not only by the thermodynamics of the casting system but also by the kinetics of the casting process. Although it is well known that polymer precipitation is due to solvent exchange with nonsolvent, with the exception of a few early studies, experimental measurements of the solvent–nonsolvent exchange rate and the additive leaching rate during polymer precipitation have been lacking. Recently, there have been many studies on the modeling of the kinetics of polymer precipitation,[18-21] but the modeling work is mainly focused on the ternary systems that constitute cellulose acetate solutions and a nonsolvent without any additives.

The present work consisted of two parts that were pertinent to the formation of asymmetric aromatic PEI membranes; the first was concerned with the study of solvent evaporation from the surface of films cast from polymer solutions, and the second with polymer precipitation of the cast films in nonsolvent water, having the final objective of getting some knowledge on the development of asymmetric PEI membranes for isopropanol dehydration by pervaporation. In the second part both the equilibrium phase separation data and the solvent–nonsolvent exchange rate, as well as the additive leaching rate, were determined.

EXPERIMENTAL

Materials

Aromatic PEI (Ultem 1000) was kindly supplied by GE Plastics Canada and was used after thorough drying at 150°C for 8 h in an oven with forced air circulation. Reagent grade *N,N*-dimethylacetamide (DMAc) and *N*-methyl-2-pyrrolidinone (NMP) were supplied by BDH Chemicals Inc. and used as received. Both solvents are miscible with water. Lithium nitrate ($LiNO_3$) from Fisher Scientific Co. was thoroughly dried before being used as an additive in the membrane casting. Water was deionized and distilled before use.

Solvent Evaporation Experiment

The solvent evaporation data were determined gravimetrically by measuring the weight change of the cast film with time. Basically, the membrane casting solution with a prescribed composition was cast on a glass plate, and then the cast polymer film, together with the plate, was immediately placed in an oven that provides a constant temperature and constant humidity. The conditions of air circulation in the oven, which affects the solvent evaporation rate, were maintained the same as in membrane preparation carried out in prior studies.[6,8] As the solvent evaporated, the weight of the plate plus the film decreased, and the change in weight was recorded as a function of time.

Polymer Precipitation Experiment

The equilibrium thermodynamic data on phase separation during polymer precipitation were determined at 25°C by the turbidimetric titration method. The polymer was dissolved in a solvent and then the polymer solution was titrated with water by means of a 0.5-mL syringe until turbidity just appeared. The turbidity was easily recognized by visual observation because of the clarity of the polymer solutions under study. During the titration procedure the polymer solution was agitated by a Teflon-coated magnetic bar. For polymer solutions of below 10 wt %, the solution viscosity was low and the turbidity point for the titration was sharply defined. For higher concentrations of polymer solutions, the mixing of the polymer solution and water was enhanced by heating the sample at an elevated temperature (60°C); if the turbidity was not observed after the sample was cooled down to the temperature of interest, namely 25°C, more water was added. To reduce solvent loss due to evaporation, rubber septa were used to isolate the samples. Because water was added dropwise with 1 drop of water being $\sim$ 0.01 g, the titration process was tedious; however, this simple method allows for systematic treatment of many samples.

The kinetic data on the polymer precipitation were obtained by in situ measurements of the solvent–nonsolvent exchange rate and the additive (if

present) leaching rate. Specifically, the solvent concentration in the gelation bath was measured as a function of time by a Beckman Total Organic Carbon Analyzer (Model 915), and the additive concentration was monitored simultaneously through conductometric measurement using a YSI Conductance Meter (Model 35) supplied by Yellow Springs Instrument Co. Inc. In taking samples for analyzing the bath-side solvent concentration, a microsyringe was used and care was exercised to minimize disturbance in the gelation bath that may otherwise be caused by the sampling.

RESULTS AND DISCUSSION

Solvent Evaporation Data

Figure 1 shows the experimental data on solvent evaporation for the casting solution of composition (in wt %): PEI(25)/DMAc(74)/$LiNO_3$(1); in the figure $(W_0 - W_t)/(W_0 - W_\infty)$ was plotted as a function of time with W_t being the weight of the cast film plus the glass plate at time t, W_0 the value of W_t at time $t = 0$, and W_∞ the value of W_t when the solvent is completely evaporated. $(W_0 - W_t)/(W_0 - W_\infty)$ is a fraction representing solvent loss due to evaporation, and this fraction develops from 0 to 1 as the evaporation proceeds.

Looking at the shape of the curve in Figure 1, the following postulations can be made. In the initial period, the cast film of polymer solution and the glass plate had temperatures lower than the equilibrium temperature, and as a result, the solvent evaporation rate increased until the equilibrium temperature was reached. Then the amount of heat transferred to the film surface was equal to the heat needed for evaporation, and the solvent loss from the film surface was compensated by solvent diffusion from the film interior to the surface, reaching a constant evaporation rate. This is characterized by the inflection point in the solvent evaporation curve. Thereafter, the solvent concentration in the film surface region dropped to a critical level because of solvent loss, and the film was solidified in the surface region, leading to a decrease in the evaporation rate. Considering that partial solvent evaporation is involved in the film formation by the dry/wet phase inversion process, an understanding of solvent evaporation in the early stages is of particular significance.

The data points in the figure, which correspond to films of the same thickness but of different surface area, fit to a single curve quite well, indicating that under the given evaporation conditions the cast film area has no appreciable effect on the solvent evaporation rate. Thus, the film area, ranging from 32 to 52 cm^2, will not be specified hereafter in presenting the solvent evaporation data. The solvent evaporation data were also determined at different temperatures for the films cast from different polymer solution compositions and with different thicknesses. The evaporation curves were found to have

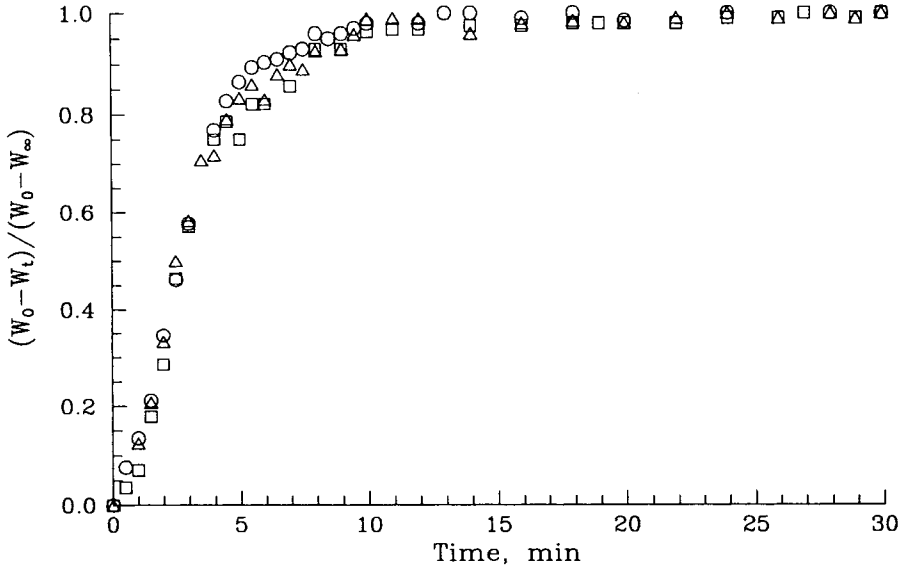

Figure 1 Experimental data on solvent evaporation. Composition of casting solution (in wt %): PEI(25)/DMAc(74)/$LiNO_3$(1). Temperature of evaporation, 90°C. Thickness of cast films, 275 μm. Area of film surface (in cm^2): (○) 53.7, (△) 21.6, and (□) 68.8.

the same features as the curve in Figure 1. It is of interest to express the solvent evaporation rate quantitatively (at least in the early stage of evaporation) in order to precisely describe the evaporation parameters that govern membrane development. While the empirical equation proposed by Kunst and Sourirajan[22] was adequate to characterize the solvent evaporation in the initial period during the formation of cellulose acetate membranes, such an expression was shown to not be applicable for the systems under study. An alternative equation, shown below, is used here,

$$\frac{W_0 - W_t}{W_0 - W_\infty} = 1 - \exp(-bt^n) \qquad (1)$$

where b and n are two empirical parameters. Rearranging eq. (1) yields

$$\log\left[-\ln\left(\frac{W_t - W_\infty}{W_0 - W_\infty}\right)\right] = n \log t + \log b \qquad (2)$$

which suggests a linear relationship between

$$\log\left[-\ln\left(\frac{W_t - W_\infty}{W_0 - W_\infty}\right)\right]$$

and $\log t$ with a slope of n and an intercept of $\log b$. This is shown in Figures 2 through 4 for all the experimental data on solvent evaporation. Thus eq. (1) is a good approximation to represent the experimental data on the solvent evaporation at the early stages, regardless of the evaporation mechanism.

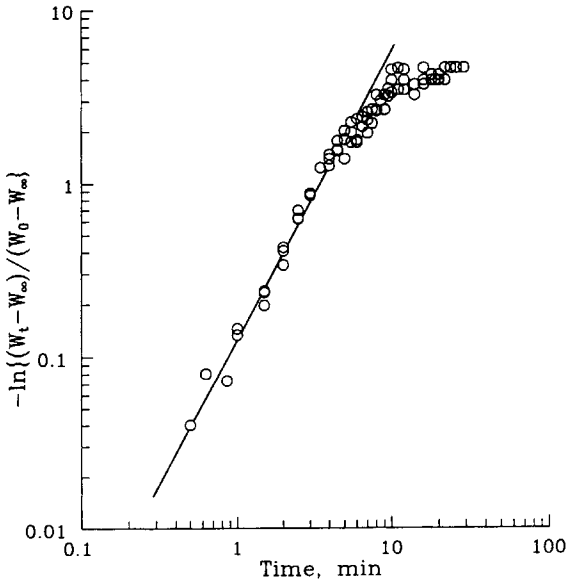

Figure 2 Logarithmic plot of $-\ln\{(W_t - W_\infty)/(W_0 - W_\infty)\}$ vs. time for the data shown in Figure 1.

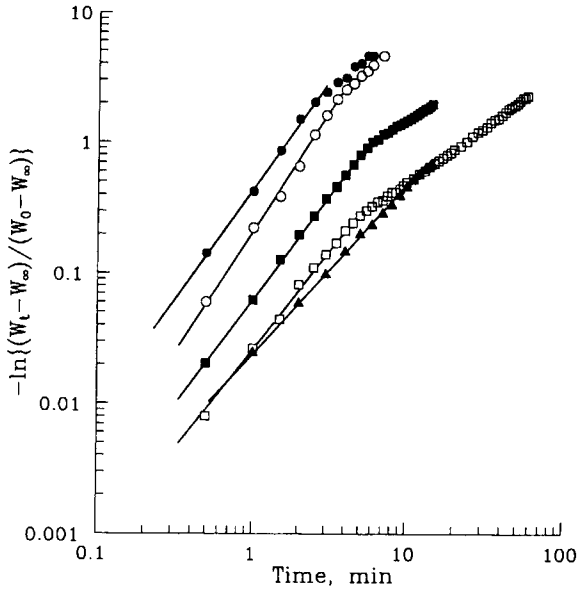

Figure 3 Logarithmic plot of $-\ln\{(W_t - W_\infty)/(W_0 - W_\infty)\}$ vs. time. Open keys represent the data of solvent evaporation at 90°C for the polymer films with different casting thickness (in μm): (○) 133, (□) 1,010; solid keys represent the data of solvent evaporation for the polymer film with a casting thickness of 275 μm at different evaporation temperatures (in °C): (●) 131, (■) 57, (▲) 32. Composition of casting solution, same as that given in Figure 1.

The numerical values of n and b are evaluated and summarized in Table I. It can be seen that for a given polymer solution composition both the values of n and b tend to increase with an increase in the evaporation temperature and/or a decrease in the film casting thickness. This is understandable because the higher the evaporation temperature and/or the thinner the film thickness is, the sooner the solvent loss reaches to the critical point for film solidification to occur. Large values of n and b characterize the fast decrease in the fractional solvent loss with time. The effect of the polymer solution composition on the evaporation parameters can best be illustrated by analyzing the data in Table I for compositions II–V; these data can be considered to be produced from a 2^2 factorial design experiment in which the polymer concentration and the additive content are two independent variables. These two variables are shown to be interacting, and the nature of the interaction is indicated by the two-way tables shown in Figure 5. At the lower level of $LiNO_3$ content (i.e., 0 wt %), an increase in polymer concentration leads to a decrease in n value and an increase

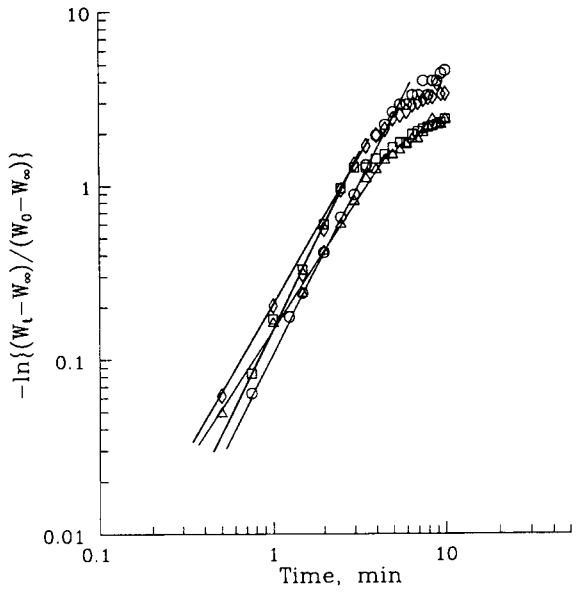

Figure 4 Logarithmic plot of $-\ln\{(W_t - W_\infty)/(W_0 - W_\infty)\}$ vs. time for the solvent evaporation data of polymer films cast from different compositions (in wt % PEI/DMAc/$LiNO_3$): (○) 20/80/0, (△) 20/78/2, (◇) 28/72/0, (□) 28/70/2. Temperature of evaporation, 90°C. Thickness of cast films, 275 μm.

in b value, whereas an increase in polymer concentration at the higher level of $LiNO_3$ content (i.e., 2 wt %) leads to an increase in n value and, with less certainty, a decrease in b value. Evidently, interaction occurs. These results partially explain the interaction effects of membrane preparation variables on the membrane performance, as identified in a previous study.[8]

The linear parts in Figures 2–4 indicate that eq. (1) is valid to describe the solvent evaporation until the solvent loss in the film reaches more than 63%, except for two cases for which the evaporation temperature is 32°C and the cast film thickness is 1,010 μm. Such a large casting thickness is rarely used in practice for membrane making, and neither is such a low evaporation temperature employed when the solvent is rather involatile. Equation (1) is thus of practical interest to quantify solvent evaporation in relation to the formation of asymmetric PEI membranes. Note that when $n = 1$, eq. (1) is identical to the equation used by Kunst and Sourirajan,[22] suggesting that eq. (1) is a more general empirical expression for solvent evaporation.

Phase Separation: Thermodynamics of Polymer Precipitation

The experimental results on the phase separation for the PEI/DMAc/H_2O system with and without $LiNO_3$ additive are shown in Figure 6 in the form of a ternary phase diagram, which consists of a boundary curve (polymer precipitation curve) distinguishing the homogeneous and the heterogeneous regions. The homogeneous liquid region lies mainly in the space between the polymer–solvent axis and the precipitation curve. This region can be considered as a measure of the system's resistance to polymer precipitation by the nonsolvent water. The size of the region is an indication of the amount of water required for the polymer precipitation to take place. It is clear from Figure 6 that for the system under study, the amount of water required to precipitate the polymer decreases with an increase in the polymer concentration, and the decrease becomes very slow when the polymer concentration is above 1 wt %. At 25°C, polymer precipitation in a polymer solution of 25 wt % needs approximately 1.5 wt % water in the absence of $LiNO_3$ additive as compared

Table I Solvent Evaporation Parameters Under Different Testing Conditions

Composition of Casting Solution (PEI/DMAc/$LiNO_3$)	Thickness of Cast Film (μm)	Temperature of Solvent Evaporation (°C)	n	b (min^{-n})
I. 25/74/1	133	90	1.813	0.206
I. 25/74/1	275	90	1.682	0.138
I. 25/74/1	1010	90	1.516	0.026
I. 25/74/1	275	32	1.281	0.024
I. 25/74/1	275	57	1.562	0.062
I. 25/74/1	275	131	1.690	0.443
II. 20/80/0	275	90	1.913	0.114
III. 20/78/2	275	90	1.535	0.148
IV. 28/72/0	275	90	1.665	0.201
V. 28/70/2	275	90	2.036	0.140

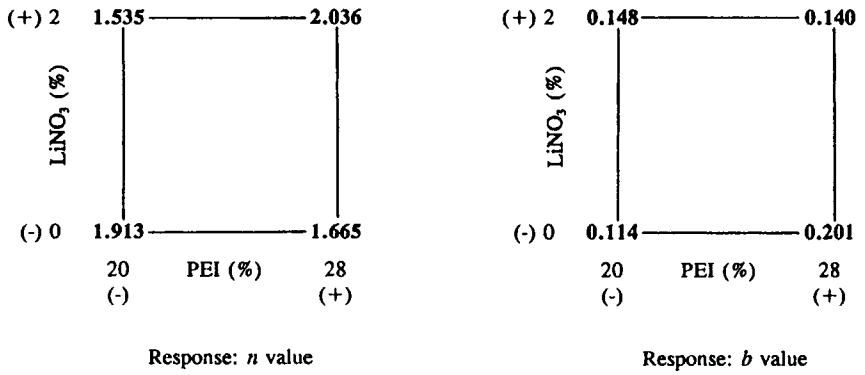

Figure 5 Two-way table illustrating the effects of casting solution composition on the solvent evaporation parameters.

to 0.5 wt % in the presence of 2 wt % $LiNO_3$. Thus the addition of $LiNO_3$ to the polymer solution reduces the tolerance for water to stay in the system before the polymer precipitates, an indication of a decrease in the dissolution power of DMAc for the aromatic PEI material. Blais[23] has reported that the potency of DMAc to dissolve aromatic polyamide was enhanced by the addition of lithium salts in the polymer solutions. The reason may be that the imide and the amide groups in the polymer chains interact with lithium salts differently. It is known that lithium salts can deactivate the hydrogen bonding sites on the amide groups and enhance the polymer solubility,[23] whereas for imide groups the lithium salts are likely to enhance the formation of polymer aggregates due to the existence of a charge transfer complex between monomeric units,[24] resulting in a reduction in polymer solubility.

NMP is another frequently used solvent for polyimides; the precipitation curves for the system PEI/NMP/H_2O were also determined at 25°C and are presented in Figure 6 for comparison. It appears that NMP is a more potent solvent than DMAc for the PEI polymer. As with DMAc as solvent, the presence of $LiNO_3$ in the PEI/NMP solutions reduces the water amount needed to induce phase separation. One may note that for a given polymer concentration the water content at the precipitation point for the systems studied here is significantly lower than the corresponding data reported by Lau et al.[25] for polyethersulfone/DMAc/water and polyethersulfone/NMP/water systems, presumably due to the fact that the sulfone group is more hydrophilic than the imide group.

The amount of water imbibed in the polymer during polymer precipitation affects the morphology of the resulting membranes directly. In casting a membrane from a given polymer, the more powerful the solvent is, the more water will be imbibed in the polymer precipitate, rendering the membrane structure more porous. Therefore, the use of an overpowerful solvent may be deleterious to the separation properties of the membrane. These considerations are supported by experimental results reported in the literature. Kneifel and Peinemann[2] found that the PEI membranes obtained by using DMAc as solvent had lower porosity than those obtained by using NMP as solvent, and Sourirajan[5] showed that DMAc was superior to NMP in preparing asymmetric PEI membranes for the selective removal of organic vapors. In practice, NMP is often used as a solvent for the preparation of a porous PEI support layer in composite membranes[2,9,26,27]; DMAc has been used as the solvent for the preparation of integral asymmetric PEI membranes for organic

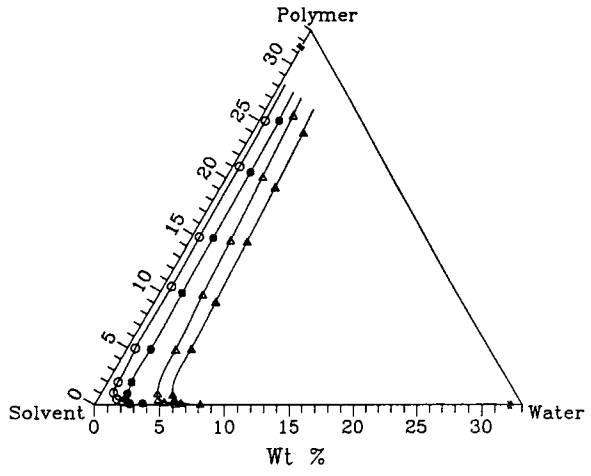

Figure 6 Phase separation data for PEI/solvent/water systems. Temperature, 25°C. Solvent, (○, ●) DMAc and (△, ▲) NMP; open keys indicate 2 wt % $LiNO_3$ present in the original polymer solution.

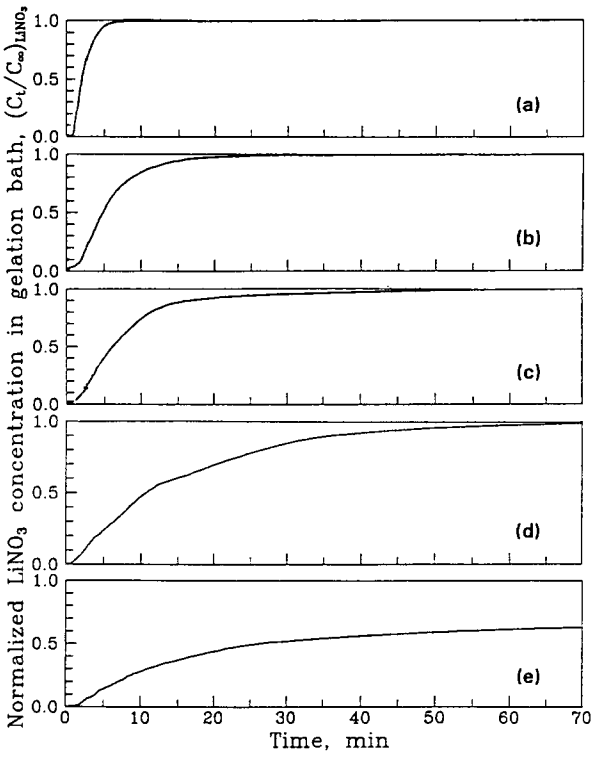

Figure 7 $LiNO_3$ additive leaching curves during polymer precipitation for the conditions given in Table II.

vapor separations[3,4] and for pervaporation applications.[6-8]

Concerning the influence of $LiNO_3$ additive on the membrane structure, two opposite effects can be distinguished from the thermodynamic point of view. On the one hand, the presence of $LiNO_3$ reduces the water amount imbibed in the polymer and hence reduces the membrane porosity. On the other hand, the additive itself contributes to the formation of pores in the membrane because it leaches out of the film during polymer precipitation. Thus the additive really acts as a "pore controller" rather than a "pore former" as it is sometimes called in the literature. The membrane morphology is apparently affected by the two opposing effects jointly.

The above discussion is based only on the equilibrium phase separation data, i.e., the thermodynamic aspect of polymer precipitation. In turbidimetric titration, as water is added to the polymer solution, the polymer–polymer intermolecular aggregation is gradually intensified. The first appearance of turbidity indicates that some polymer aggregates have began to come out of the solution due to phase separation. In the membrane making processes, however, the cast polymer film is immersed in a water bath, a situation which has the features of fast titration of polymer solution by water and overshooting of the titration by an excess amount of water. Therefore, care must be exercised in applying the thermodynamic results obtained from titration experiments to the membrane development because of the difference in the process details.

Kinetics of Polymer Precipitation

The kinetics of polymer precipitation is characterized here by the solvent–nonsolvent exchange rate and the additive leaching rate, which were obtained experimentally by following the composition change in the gelation bath. Figure 7 shows the bath-side $LiNO_3$ concentration vs. time under the different conditions specified in Table II.

The highest $LiNO_3$ concentration encountered in the measurements was 5.7 ppm, in which concentration range a linear increase in conductance with $LiNO_3$ concentration was observed. The presence of DMAc (with a maximum concentration of 143 ppm) in the gelation bath due to solvent exchange with nonsolvent was found to have essentially no effect on the conductance measurement. Therefore, the conductance readings can readily be converted into $LiNO_3$ concentration data, and for convenience the relative concentration $(C_t/C_\infty)_{LiNO_3}$ was used in Figure 7 with C_t and C_∞ denoting, respectively, the concentration at time t and at infinite time when the concentration reaches a constant.

It should be noted that after being immersed in the gelation bath, the cast film soon separated from the glass plate, and then the solvent–nonsolvent exchange and the additive leaching began to occur on both sides of the film. There is a time lag in the

Table II Conditions for Kinetic Measurement of Polymer Precipitation

	a	b	c	d	e
Casting solution composition (PEI/DMAc/$LiNO_3$)	25/74/1	20/79/1	25/74/1	25/74/1	25/74/1
Casting thickness (μm)	275	275	275	532	275
Evaporation conditions	—	—	—	—	90°C, 2 min
Gelation temperature (°C)	45	18	18	18	18

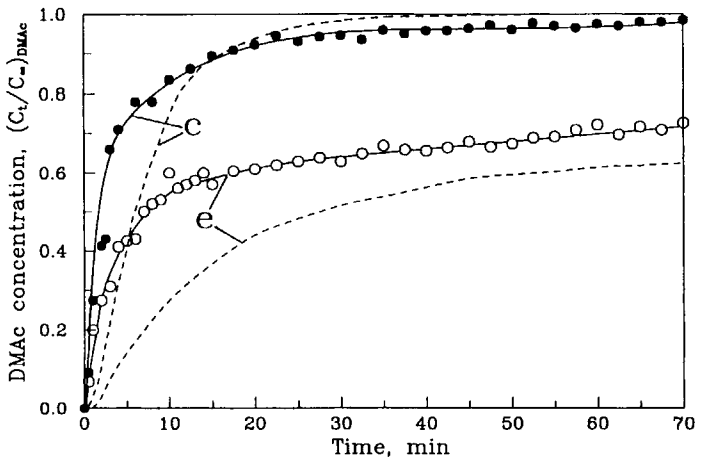

Figure 8 Solvent–nonsolvent exchange curves during polymer precipitation. Letter codes in the figure indicate the conditions given in Table II. For comparison the corresponding $LiNO_3$ leaching curves are shown by the dotted lines.

$LiNO_3$ leaching curves early in the beginning, which is due to the fact that the probe (dip-cell) for conductance measurement was not located exactly on the membrane surface and it takes time for $LiNO_3$ molecules leaching out of the film to reach the probe. Although the concentration measured was not really the membrane–bath interfacial concentration, the leaching curves are still valid to show the following qualitative trends because the probe was fixed at a given position near the membrane surface in all the measurements:

1. As gelation proceeds, the rate of $LiNO_3$ leaving the film decreases, as shown by the concave of the leaching curves toward the time axis.
2. By comparing Figures 7(a)–(d) it is shown that the $LiNO_3$ leaching rate decreases with a decrease in gelation temperature, an increase in polymer concentration in the casting solution, and an increase in membrane casting thickness.
3. Comparison of Figures 7(c) and (e) shows that when the cast film undergoes a solvent evaporation step, the $LiNO_3$ leaching rate in the subsequent gelation step will be decreased significantly.

These results are understandable because $LiNO_3$ within the cast film has to diffuse through the gelled polymer layer at the interface between the film and the gelation medium. The gelled polymer layer, whose thickness increases during the polymer precipitation period, acts as a barrier to the additive leaching. The leaching rate gives some information concerning the morphology and structure of the films so formed which have significant effects on the membrane permselectivity. Fast leaching of the additive is an indication of the porous structure of the membrane, and a sharp decrease in the leaching rate with time is an indication of the structural gradient in the membrane. The trends similar to additive leaching are naturally expected for the diffusive exchange between solvent and nonsolvent. Note that despite the smaller molecular size of $LiNO_3$ compared to that of DMAc, the solvent–nonsolvent exchange rate is faster than the $LiNO_3$ leaching rate at the initial stage of gelation, as shown in Figure 8. The reason may be that as $LiNO_3$ within the films leaches out, the gelation medium (nonsolvent) moves in, and consequently the solvent–nonsolvent contact is enhanced. Figure 8 also shows that when the gelation proceeds with time to some extent, the percentage DMAc flowing out of the film becomes smaller than $LiNO_3$, eventually resulting in a situation where $LiNO_3$ leaching has finished whereas the solvent–nonsolvent exchange is not yet complete.

CONCLUSIONS

Studies were carried out on the solvent evaporation and polymer precipitation pertinent to the formation of asymmetric PEI membranes using the dry/wet phase inversion technique. Experimental data of solvent evaporation from the surface of freshly cast films were obtained. It was found that solvent evaporation in early stages could be expressed quantitatively by an empirical equation containing two

parameters. Analysis of the evaporation parameters provided a partial explanation for the interaction effect of membrane preparation variables on membrane performance. The equilibrium phase separation data for PEI/DMAc/H_2O and PEI/NMP/H_2O systems with and without $LiNO_3$ additive were determined. The solvent–nonsolvent exchange rate and the additive leaching rate during polymer precipitation in nonsolvent water were measured. These data were discussed with reference to the formation of asymmetric PEI membranes. It was also shown that the presence of $LiNO_3$ additive in the membrane casting solution influenced not only the solvent evaporation rate in the dry step, but also the thermodynamic as well as the kinetic aspects of polymer precipitation in the subsequent wet step.

The authors acknowledge financial support by the Institute for Chemical Science and Technology and by the Natural Science and Engineering Research Council of Canada.

REFERENCES

1. K.-V. Peinemann, K. Fink, and P. Witt, *J. Membr. Sci.*, **27,** 215 (1986).
2. K. Kneifel and K.-V. Peinemann, *J. Membr. Sci.*, **65,** 295 (1992).
3. X. Feng, S. Sourirajan, F. H. Tezel, T. Matsuura, and B. A. Farnand, *Ind. Eng. Chem. Res.*, **32,** 533 (1993).
4. S. Deng, S. Sourirajan, T. Matsuura, and B. A. Farnand, in *Proceedings of the Sixth International Conference on Pervaporation Processes in the Chemical Industry,* R. Bakish, Ed., Bakish Materials Corp., Englewood, NJ, 1992, pp. 504–513.
5. S. Sourirajan, *A Study of Volatile Hydrocarbon Emission Control by Membranes,* Report submitted to Energy, Mines and Resources Canada under DSS Contract No. 23440-9-9237/01 SS, September 1991.
6. R. Y. M. Huang and X. Feng, *Sep. Sci. Technol.*, **28,** 2035 (1993).
7. R. Y. M. Huang and X. Feng, *J. Membr. Sci.*, **84,** 15 (1993).
8. X. Feng and R. Y. M. Huang, *J. Membr. Sci.*, to appear.
9. J. Bai, A. E. Fouda, T. Matsuura, and J. D. Hazlett, *J. Appl. Polym. Sci.*, **48,** 999 (1993).
10. S. Loeb and S. Sourirajan, *Sea Water Demineralization by Means of Semipermeable Membranes,* Department of Engineering, University of California, Los Angeles, Report No. 60-60, 1960.
11. J. Neel, in *Pervaporation Membrane Separation Processes,* R. Y. M. Huang, Ed., Elsevier Science Publishers, Amsterdam, 1991, pp. 1–109.
12. L. Yilmaz and A. J. McHugh, *J. Membr. Sci.*, **28,** 219 (1986).
13. W. B. Krantz, R. J. Ray, R. L. Sani, and K. J. Gleason, *J. Membr. Sci.*, **29,** 11 (1986).
14. C. S. Tsay and A. J. McHugh, *J. Membr. Sci.*, **64,** 81 (1991).
15. S. B. Tantekin, W. B. Krantz, and A. R. Greenberg, *Polym. Prepr.*, **30**(1), 36 (1989).
16. M. Ataka and K. Sasaki, *J. Membr. Sci.*, **11,** 11 (1982).
17. S. Sourirajan and T. Matsuura, *Reverse Osmosis/Ultrafiltration Process Principles,* National Research Council Canada, Ottawa, 1985.
18. A. J. Reuvers and C. A. Smolders, *J. Membr. Sci.*, **34,** 67 (1987).
19. C. S. Tsay and A. J. McHugh, *J. Polym. Sci., Polym. Phys. Ed.*, **28,** 1327 (1990).
20. C. S. Tsay and A. J. McHugh, *J. Polym. Sci., Polym. Phys. Ed.*, **29,** 1261 (1991).
21. C. S. Tsay and A. J. McHugh, *J. Polym. Sci., Polym. Phys. Ed.*, **30,** 309 (1992).
22. B. Kunst and S. Sourirajan, *J. Appl. Polym. Sci.*, **14,** 1983 (1970).
23. P. Blais, in *Reverse Osmosis and Synthetic Membranes. Theory-Technology-Engineering,* S. Sourirajan, Ed., National Research Council Canada, Ottawa, 1976, pp. 167–210.
24. A. Viallat, J. P. C. Addad, R. P. Bom, and S. Perez, *Polymer,* **33,** 2784 (1992).
25. W. W. Y. Lau, M. D. Guiver, and T. Matsuura, *J. Membr. Sci.*, **59,** 219 (1991).
26. C. P. Borges, M. H. V. Mulder, and C. A. Smolders, in *Proceedings of the Sixth International Conference on Pervaporation Processes in the Chemical Industry,* R. Bakish, Ed., Bakish Materials Corp., Englewood, NJ, 1992, pp. 207–222.
27. S. Gagne, K. Volchek, D. Velicogna, R. K. Tyagi, and T. Matsuura, in *Proceedings of the Sixth International Conference on Pervaporation Processes in the Chemical Industry,* R. Bakish, Ed., Bakish Materials Corp., Englewood, NJ, 1992, pp. 411–422.

Received March 18, 1994
Accepted February 7, 1995